Tomographic Processing of Spotlight-Mode SAR

Collection Editor:
Jason Ryan

Tomographic Processing of Spotlight-Mode SAR

Collection Editor:
Jason Ryan

Authors:
Aaron Hallquist
Tianlai Lu
Jason Ryan

Online:
< http://cnx.org/content/col10498/1.1/ >

C O N N E X I O N S

Rice University, Houston, Texas

Collection structure revised: December 19, 2007
PDF generated: February 4, 2011
For copyright and attribution information for the modules contained in this collection, see p. 29.

Table of Contents

Chapter 1

Introduction[1]

1.1 Introduction

Our project covers an investigation of Synthetic Aperture Radar (SAR) and the Matlab processing of SAR data we received from Ohio State University. The data was generated by a simulation of spotlight-mode SAR, a specific type of SAR which takes advantage of a moving sensor tracking a single ground target. To process this data, we utilize digital signal processing techniques such as interpolation and windowing along with a knowledge of how SAR works.

[1] This content is available online at <http://cnx.org/content/m15658/1.1/>.

Chapter 2

Background[1]

2.1 Synthetic Aperture Radar: Background

2.1.1 What is Synthetic Aperture Radar?

Synthetic Aperture Radar (SAR) is a microwave imaging system that is used to obtain high resolution pictures of large areas of terrain. The radar can be either airborne or spaceborne. As the platform moves, closely spaced pulses are transmitted and the reflected signals are received and processed using Fourier methods. The processed data resembles data taken with a system that has a very large antenna, thus allowing extremely high resolution.

Synthetic Aperture Radar was first developed in the early 1950's. The earliest type of SAR is called strip-mapping mode SAR. It is primarily used for imaging large areas of terrain, such as the surface of a nearby planet. This mode emits the radar pulses at a constant "look" angle to the surface while traveling along a flight path or orbit. This process creates a strip of mapped ground, and can be repeated along a polar orbit to map the entire surface of a planet.

Spotlight mode SAR is a newer form of SAR and was developed in the early 1980's. It is more widely used today than strip-mapping mode and it is what our project deals with. In spotlight mode, the radar is steered continually as the carrier of the radar flies over a patch of ground. In another word, the "look" angle is constantly adjusted so that a single patch of ground is always illuminated. This method allows for higher resolution in the azimuth "travel" direction of the platform but is not able to image as large of an area as strip-mapping mode.

2.1.2 How Does Imaging Radar Work?

As mentioned earlier, we use the Synthetic Aperture Radar processing technique because of its advantages when it comes to imaging large areas at high resolutions. However, why do we even use radar to image things in the first place?

Radar is used in imaging because of the minimal constraints that is has on time-of-day and atmospheric conditions. The area of imaging does not have to be illuminated by sunlight in order to obtain a picture. This allows for continuous mapping regardless of the position of the sun, which saves time and therefore, money.

Radar also has the ability to penetrate cloud cover because one can choose a wavelength that is not absorbed by water. This fact is what allowed scientists at NASA to provide stunning images of the surface of Venus, which is completely shrouded in cloud-cover.

Imaging radar works by emitting a signal and then recording the strength of the reflected signal (scattering coefficient) for that area. The pulses are emitted at an angle to the surface such that if they strike a smooth,

[1] This content is available online at <http://cnx.org/content/m15667/1.1/>.

flat surface, very little of the signal will be reflected back towards the antenna which corresponds to a darker spot on our scattering coefficient image.

When the radar pulse strikes uneven surfaces such as urban areas or vegetated areas, the signal gets reflected numerous times and there is an increased likelihood that the radar antenna will eventually receive a large portion of the signal back, corresponding to a whiter spot on your image. Scientists use this fact to determine the extent of flooding in urban areas or to discern how much an oil spill in the ocean has grown.

2.1.3 Synthetic Aperture Radar and Microwave Imaging System

The resolution of an image taken from an imaging system is usually determined by the size of the Aperture (lens for optical systems and antenna for radar). Conventional radar systems use passive methods deployed with optical or short-wave infrared sector that rely on sunlight reflection. On the other hand, synthetic Aperture Radar uses a microwave imaging system. Two important advantages resulting from using microwave pulses are that cloud cover can be penetrated and the imaging process can be performed at night.

However, antenna size limits one from applying microwave imaging systems. A very large size of antenna is required to obtain satisfactory resolution. Therefore, the size of the antenna makes it impractical for the radar carrier.

Synthetic Aperture Radar solves the problem by "simulating" a large Aperture. The radar sends and receives signals from a relatively small antenna while the platform traveling along a flight path. One can then use the digital signal processing techniques to combine the data into a coherent image. The result is the same as if one has used a very large antenna.

Chapter 3

Projection-Slice Theorem[1]

3.1 Brief Review of Computer-Aided Tomography

Computer-Aided Tomography, or CAT (as in CAT scan) is a technique for remote 2-D and 3-D imaging. By moving a sensor around a target, one can collect sufficient 1-dimensional data to reconstruct the original multidimensional image. This process utilizes an amazing relationship called the Projection-Slice Theorem, which states that each piece of projection data at some angle is the same as the Fourier transform of the multidimensional object at that angle. Using a range of data from a range of angles, one can, given sufficient computation resources, reconstruct the actual image by taking the inverse transform. The Projection-Slice Theorem has found a range of applications in remote sensing, the most famous of which is the 3-D imaging of humans, popularly known as the CAT scan. The focus of this project, Spotlight-Mode Synthetic Aperture Radar, uses the Projection Slice Theorem in a way quite similar to CAT scan technology, except the way radar projections are generated by the image is slightly different from the way CAT scans use X-rays.

3.1.1 Projection-Slice Theorem

Let g(x,y) represent the radar reflection of our image. The two-dimensional Fourier transform of g is defined as

$$G(x,y) = \int_{-\infty}^{\infty} \int_{-\infty}^{\infty} g(x,y) e^{-j(xX+yY)} \, dx \, dy$$

Figure 3.1

And

[1] This content is available online at <http://cnx.org/content/m15663/1.1/>.

$$g(x,y) = \frac{1}{4\pi^2}\int_{-\infty}^{\infty}\int_{-\infty}^{\infty} G(x,y)e^{j(xX+yY)}dXdY$$

Figure 3.2

We can model the reflection behavior of the incident radar by considering the following overhead diagram

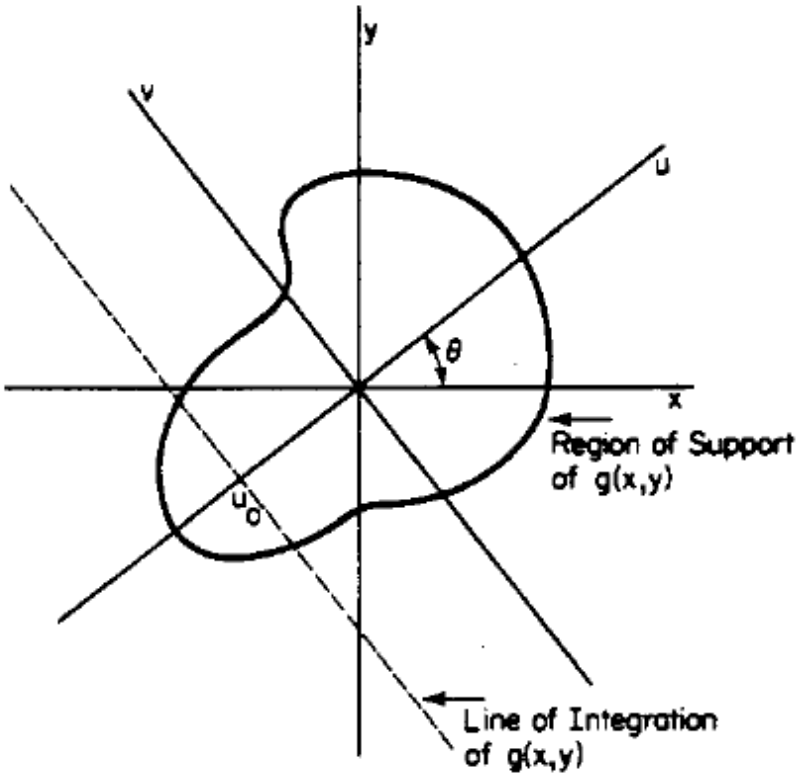

Figure 3.3

The smooth line outlines our image g(x,y), and the horizontal and vertical axes x,y are overlaid. The radar is incident upon the target along the axis of the path **u** at an angle theta. For a target which is far away, the radar wave front is approximately flat, and so this means that a reflected beam which has traveled a certain unique distance to and from the sensor comes from a straight path across the image, perpendicular to **u**. This path is in the direction of **v** and can be represented by a line integral in the direction of **v** at position **u0**. The formula for this is given by

$$p_\theta(u) = \int_{-\infty}^{\infty} g(u\cos\theta - v\sin\theta, u\sin\theta + v\cos\theta)\, dv$$

Figure 3.4

The 1-D Fourier transform of **p(u)** is given by

$$P_\theta(U) = \int_{-\infty}^{\infty} p_\theta(u) e^{-juU}\, du$$

Figure 3.5

And then, through applying the equation for **p(u)** and simplifying, we are left with

$$P_\theta(U) = G(U\cos\theta\,, U\sin\theta)$$

Figure 3.6

This is the Projection Slice Theorem! What this states is that the Fourier transform of a projection taken at an angle theta is **equal to** the 2-D Fourier transform of the image at that same angle theta. To reconstruct the original image, one must merely take the inverse Fourier transform in two dimensions of a set of data **P(U)**. This is not as easy as it sounds for reasons discussed later. Notice how the Fourier transform of the image **G** does not have the usual form, **G(X,Y)**. It is instead expressed in polar form, and the variable theta lets us know that we have only a slice of the transform for each P(U).

Chapter 4

Tomographic Processing[1]

4.1 Data Processing

In the words of the highly esteemed Rich Baraniuk, the signals received by the radar sensor must be "munjed" upon in order that the user can learn anything useful at all. We flesh-out the basic spotlight-mode SAR derivation from start to finish, noting the places in which we make approximations, all the while aiming at interpreting our bit stream into the meaningful pieces of the Projection-Slice Theorem. Something to note is that this theoretical approach does not include any Doppler shift analysis. Other approaches to synthetic aperture radar heavily rely on phase data collected during a physical flyby of the target, where instrument velocity plays an important role. The mathematics in this section follows as in David Munson's 1983 paper on "A Tomographic Formulation of Spotlight-Mode Synthetic Aperture Radar."

4.1.1 The Setup

The way spotlight-mode SAR collects data samples is by gathering image projections from a range of angles. In our case, this range is broken down into a set of equally spaced angles so that essentially we have snapshots at various views around a target. A depiction of what it would look like is given below.

[1] This content is available online at <http://cnx.org/content/m15661/1.1/>.

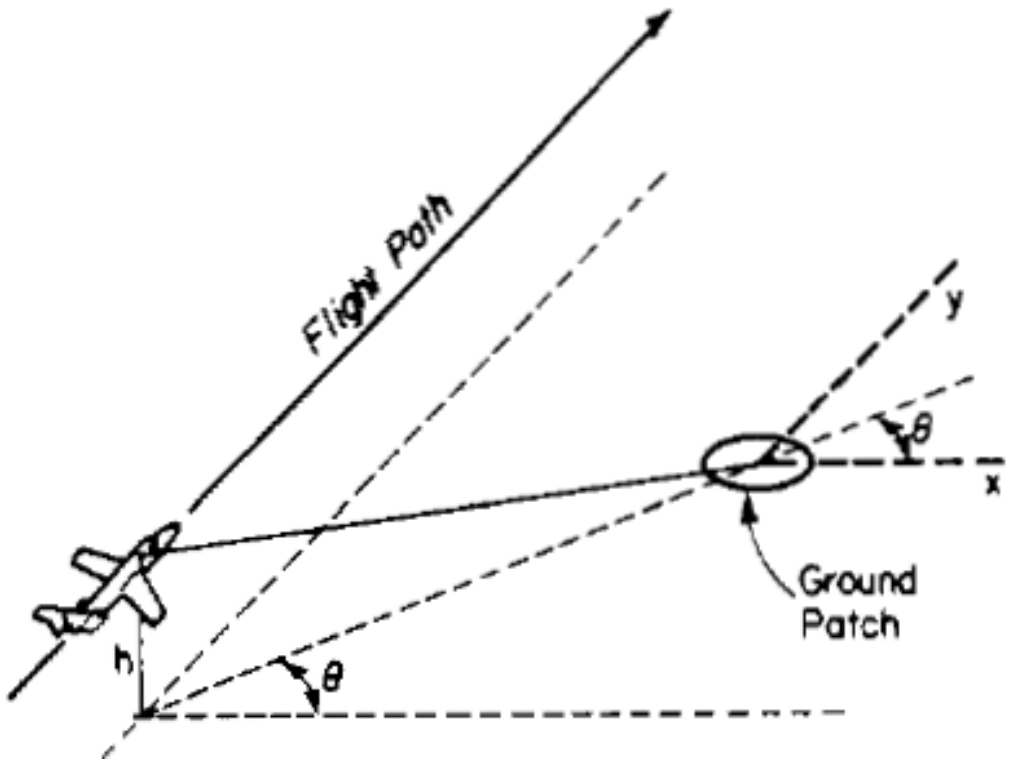

Figure 4.1

This drawing shows how the altitude of the sensor platform might play a role in the angular view of the target. For our derivation, we will ignore this parameter and assume that the radar is somehow incident at ground level, that as the sensor moves closer to the target distances remain undistorted by this variation in 3-dimensions. This ground plane geometry is as shown below.

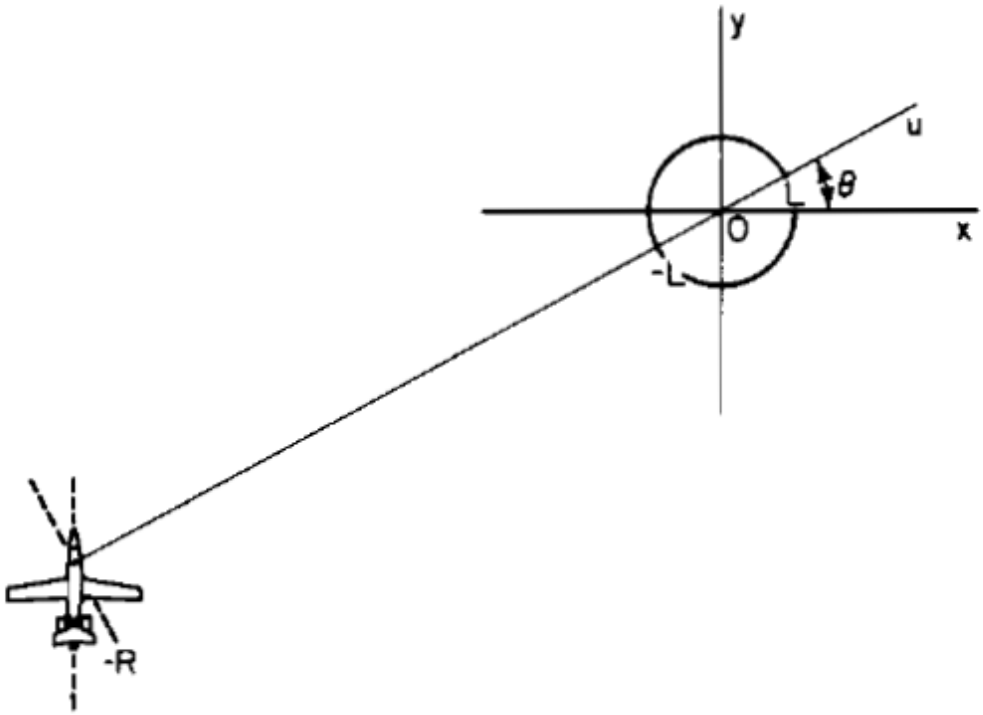

Figure 4.2

Note that the angle **theta** is the same as that in the description of the Projection-Slice Theorem. The distance from the center of the target image is given by the variable **R**, and the radius of a circular target is given by **L**. The radar signal travels along and parallel to path **u**.

4.1.2 Generating the Reflection Signal

At this point we are ready to start generating our signals! Our radar device works in a microwave frequency range designed to penetrate clouds and other obstructions with ease. It emits a linear FM chirp pulse waveform **Re{s(t)}** where

$$s(t) = \begin{cases} e^{j(\omega_0 t + at^2)}, |t| \leq \frac{T}{2} \\ 0, \quad otherwise \end{cases}$$

Figure 4.3

In this signal, **w0** is the RF carrier frequency and **2a** is the FM rate. The frequency rises linearly with time so that the minimum frequency is **w0-aT** and the maximum is **w0+aT**. The point reflection off of a reflection coefficient at **(x0,y0)** given by **g(x0,y0)** can be written

$$r_0(t) = A \cdot Re\left\{g(x_0, y_0)s(t - \frac{2R_0}{c})\right\}dxdy$$

Figure 4.4

Where **R0** is the distance of **g(x0,y0)** from the radar, A accounts for propagation attenuation, **c** is the speed of light, and **2R0/c** accounts for the two-way travel time from radar to target.

4.1.3 Interpreting the Reflection Signal

Points on the target ground patch equidistant from the radar lie on an arc, but typically **R≫L**, so this arc is nearly, and may be approximated as, a straight line. Combining this approximation with the polar formulation of a differential line of scatterers (radar reflectors), we can write down a new relation involving a polar representation of the reflection.

$$r_1(t) = A \cdot Re\left\{p_\theta(u_0)s\left(t - \frac{2(R + u_0)}{c}\right)\right\}du$$

Figure 4.5

If **R≫L**, we may take **A** as a constant over **u**, and this enables us to write the reflection from the whole ground patch as the integral of **r1** over **u**.

$$r_\theta(t) = A \cdot Re\left\{\int_{-L}^{L} p_\theta(u)s\left(t - \frac{2(R + u)}{c}\right)du\right\}$$

Figure 4.6

This integral has the form of a convolution! This provides us a good hint that Fourier methods might be the right way to analyze this signal. The signal stated here is really the raw data that we receive from the radar. The return chirp is the projection slice convolved with the initial pulse.

4.1.4 Mixing the Reflection Signal

It turns out that the correct way to process this raw data is to mix it with the starting signal, **s(t)**. Written out, **r(t)** has the form

$$r_\theta(t) = A \cdot Re\left\{\int_{-L}^{L} p_\theta(u) \exp\left\{j\left[\omega_0\left(t - \frac{2(R+u)}{c}\right) + a\left(t - \frac{2(R+u)}{c}\right)^2\right]\right\} du\right\}$$

Figure 4.7

$$-\frac{T}{2} + \frac{2(R+L)}{c} \leq t \leq \frac{T}{2} + \frac{2(R-L)}{c}$$

Figure 4.8

Mixing this signal with the real and imaginary parts of the signal **s(t)**, low-pass filtering the two, and then adding them together gives us a complex signal.

$$C_\theta(t) = \frac{A}{2}\int_{-L}^{L} p_\theta(u) \exp\left\{j\frac{4au^2}{c^2}\right\} \cdot \exp\left\{-j\frac{2}{c}\left(\omega_0 + 2a\left(t - \frac{2R}{c}\right)\right)u\right\} du$$

Figure 4.9

The quadratic term in the exponential can be approximated as 0, and as that term disappears, we get a very profound result

$$\overline{C}_\theta(t) = \frac{A}{2}\int_{-L}^{L} p_\theta(u) \exp\left\{-j\frac{2}{c}\left(\omega_0 + 2a\left(t - \frac{2R}{c}\right)\right)u\right\} du$$

Figure 4.10

Which is the Fourier transform of **p(t)**.

$$\bar{C}_\theta(t) = \frac{A}{2} P_\theta \left[\frac{2}{c} \left(\omega_0 + 2a \left(t - \frac{2R}{c} \right) \right) \right]$$

Figure 4.11

4.1.5 Interpreting Our Result

From our formulation of **r(t)** above, we know the restriction on **t**. If we consider the argument of **P( )** to be **X**, the radial spatial frequency, we know **P(X)** is only determined for **X** between **X1** and **X2** where

$$X_1 = \frac{2}{c} \left(\omega_0 - aT + \frac{4aL}{c} \right)$$

Figure 4.12

$$X_2 = \frac{2}{c} \left(\omega_0 + aT - \frac{4aL}{c} \right)$$

Figure 4.13

The term **4aL/c** will be negligible for typical SAR, so we can see that **X1** and **X2** are proportional to the lowest and highest frequencies in the transmitted chirp pulse. **X1** and **X2** correspond to the inner and outer radii for which **P(X)** is defined.

$$\frac{2}{c}(\omega_0 - aT) \leq X \leq \frac{2}{c}(\omega_0 + aT)$$

Figure 4.14

C(t) is the final form of the processed data! What this tells us is that after mixing the reflection with the real and imaginary parts of the original chirped pulse, low-pass filtering, and linearly combining the two, we are left with the Fourier transform of the projection **p(t)**. From here we need to take the inverse transform

to finally reconstruct **g(x,y)**. Unfortunately, we have the polar form of a Fourier transform, whose known values would be located somewhere on this Locus

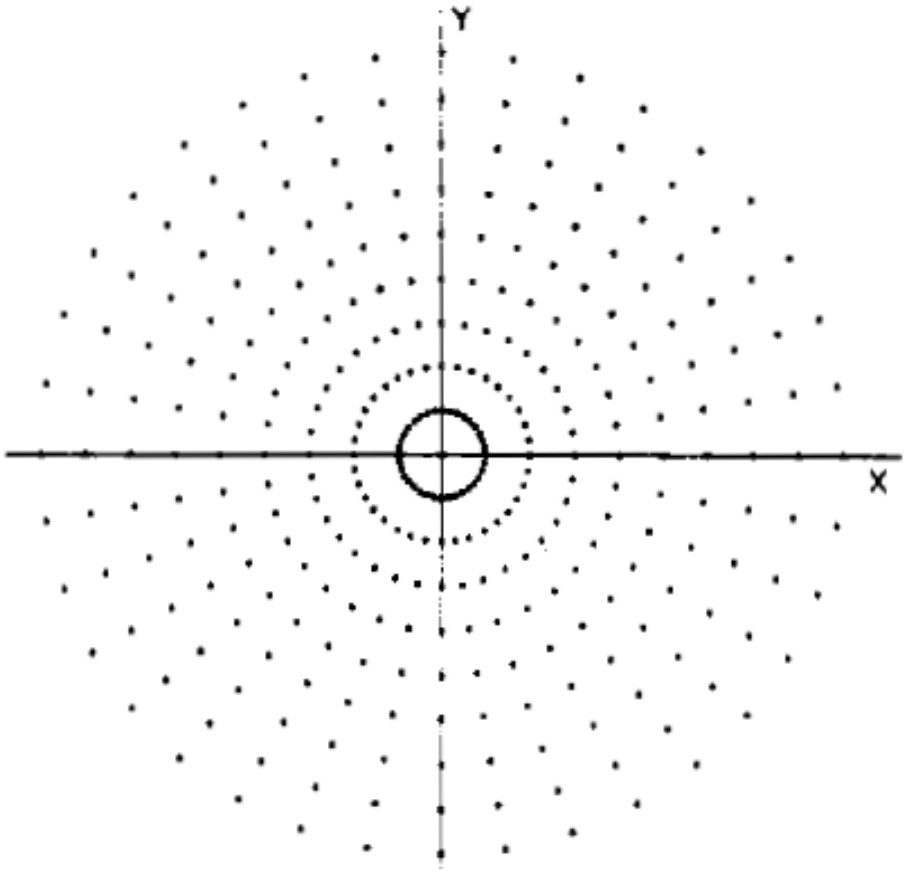

Figure 4.15

There exists a 2-D polar inverse Fourier transform, and this is the preferred method of transform for the optimal quality reconstruction. This method, called Convolution Back-Projection, requires an enormous number of computations to execute, however, and so in practice one has to either have a quite powerful system or be ready to wait for results. The practical method attempts to remedy this issue by utilizing the Fast Fourier Transform, or FFT. Although there is no known 2-dimensional FFT or inverse FFT for polar coordinates, one may interpolate the polar data to rectify the coordinate system and then apply the 2-D inverse FFT in the regular fashion. The rectification process requires windowing the data, and interpolation is by its nature inexact, so this method ends up trading a great deal of resolution for extra speed.

Chapter 5

Data and Processing[1]

5.1 Introduction and Preparation of SAR Data

In order to simulate the processing of SAR data, we received SAR data from the ECE department at Ohio State University. The data they gave us was acquired through a computer simulated fly-by past a CAD model of a backhoe.

Figure 5.1

The data we received from OSU was in digital format, meaning the analog mixing and low pass filtering was already completed and we received digitized versions of $C\theta(t)$. This function was shown to be equivalent to $P\theta(U)$, the Fourier transform of our projection slices $p\theta(u)$. The matlab file that contained this information was a 512x1541 matrix iq_lin, a vector of various $P\theta$ signals for different values of θ, the viewing angle. There were 1541 different viewing angles, listed in az_lin, that stepped by $1/14^\circ$ for each element and varied from -10° to 100°, a median viewing angle of 45°. We also received a vector of length 512 called f that contained the microwave frequencies (7-13 GHz) that were transmitted and received. By using the wideband approximation, we made the transformation from time frequency to spatial frequency via

$R \approx 2\omega/c = (4\pi/c)\, f$

where R is the radial spatial frequency and f is the microwave frequency content. By the projection slice theorem, we have that the various $P\theta$ are arranged radially in a polar grid along the various angles θ. We

[1] This content is available online at <http://cnx.org/content/m15659/1.1/>.

then get that our data lies on a domain
$-10^\circ \leq \theta \leq 100^\circ$
$R \in \Delta\mathrm{R} = [(4\pi/c)\, f_{\min}, (4\pi/c)\, f_{\max}]$

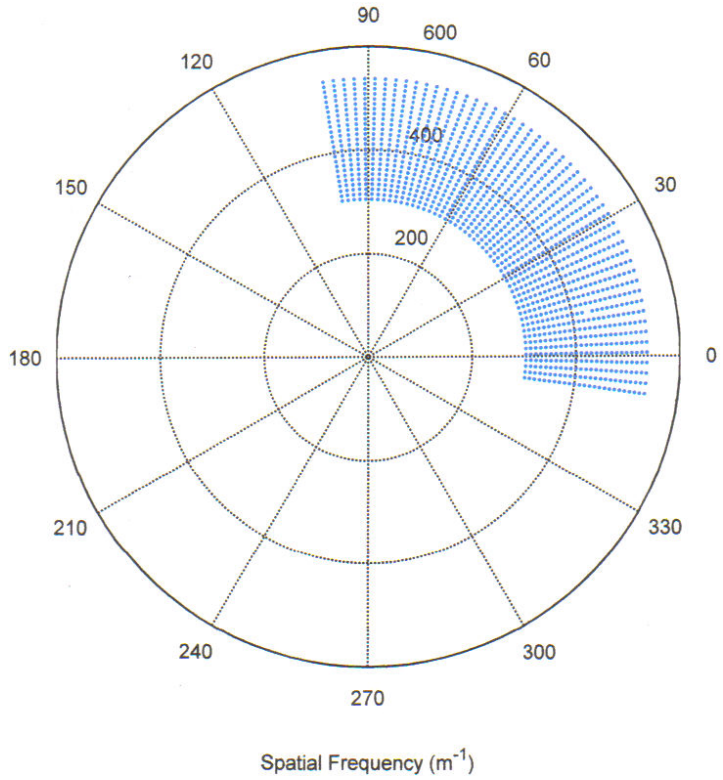

Figure 5.2

5.2 Processing of SAR Data

Knowing that our data is the Fourier transform of our image, after the proper preparation we want to take the inverse Fourier transform. To do this simply and efficiently (we don't want Matlab running for hours!) we linearly interpolate the data to a Cartesian grid. This is done in our Matlab function sar_lin (code found in appendix). The idea is to find an inscribed rectangular grid inside our polar data. We chose to use the square centered at 45° inscribed in our ribbon. To interpolate we made a Cartesian grid at this location and computed the polar representation of each point in order to find its 4 nearest polar neighbors. Once those neighbors were found, the Cartesian point's value was determined by linearly interpolating in the R-direction for the two θ values and then linearly interpolating in the θ-direction. The end result of our program's running of this is shown below.

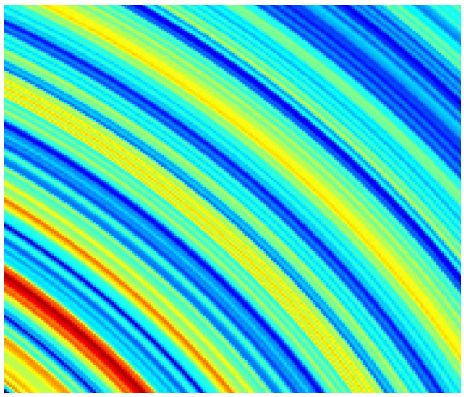

Figure 5.3

After linearly interpolating each point in the Cartesian grid we have formed, we now have our data in a form that allows us to take the 2-d inverse DFT by the fast Fourier transform method. This is what saved us computation time (program ran in about 15 seconds) and is the reason we interpolated to Cartesian coordinates to begin with. Below is the image after taking the inverse Fourier transform.

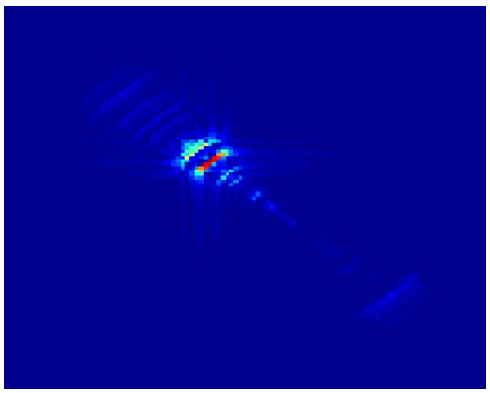

Figure 5.4

Chapter 6

Conclusions and Future Work[1]

6.1 Conclusions

Our project shows that an image can be extracted from scattering coefficients obtained from SAR techniques. One need only apply some digital signal processing techniques, such as the polar to Cartesian interpolation of our data. SAR has many benefits and real world applications. For example, the microwave radiation used in SAR penetrates cloud cover. This fact has been used to image Venus' surface, providing stunning visuals otherwise unavailable. Another benefit is that SAR does not require the construction of a large antenna as the motion of the detector creates an artificial aperture.

6.2 Future Work

One negative aspect of our data is that the range of frequencies represented is very narrow. That is, the interpolated grid we chose focuses on a small range of frequencies relative to the amount of data that we received to work with. One potential fix for this is to do multiple interpolations of multiple Cartesian grids, ensuring no overlap, and superimpose the images that result. As long as the relative location of the grids is taken into account, then by linearity, we should be able to acquire a more detailed image by superimposing the images. One might imagine, for example, that we could superimpose the grids shown below.

[1] This content is available online at <http://cnx.org/content/m15660/1.1/>.

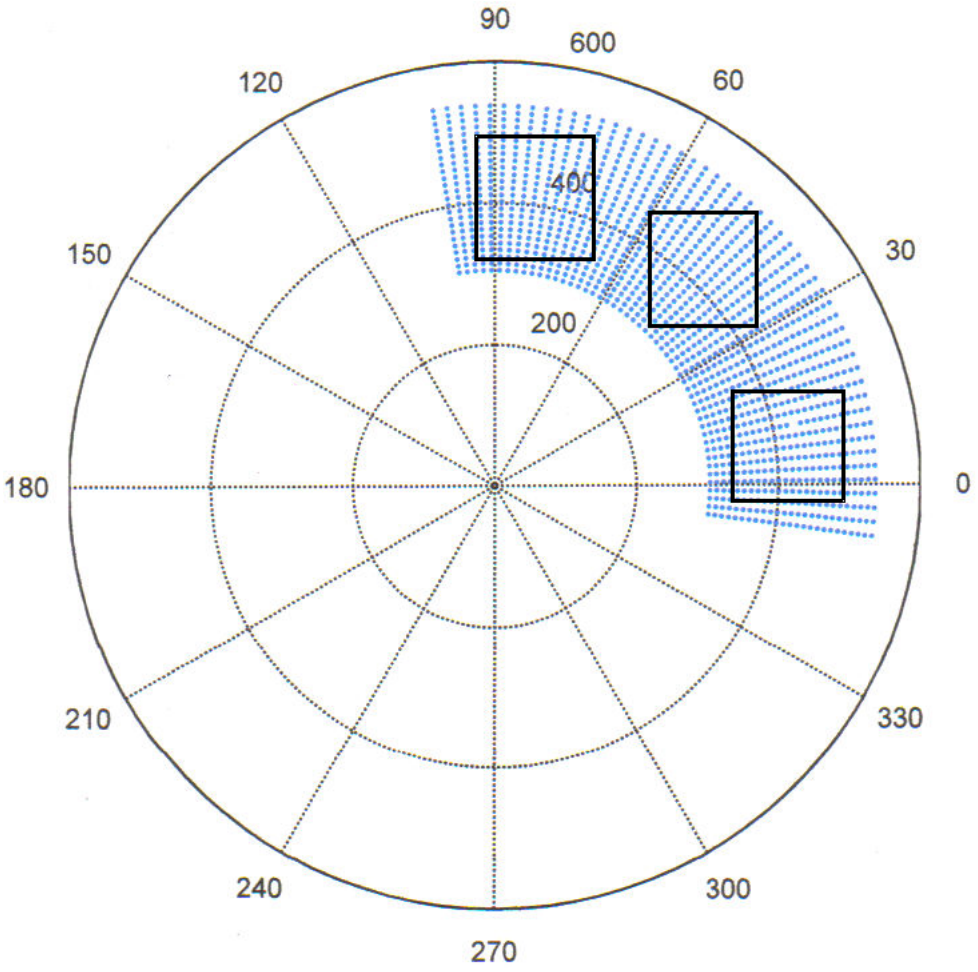

Figure 6.1

Another possibility is to forego the interpolation, which restricts the amount of data that we can use, and instead we can work in polar coordinates. This would allow us to use all of our data, cutting out nothing. The downside to this is that there is no fast Fourier transform method for polar coordinates, so the computational complexity increases the run time to be on the order of hours.

Chapter 7

Appendix and References[1]

7.1 Appendix

7.1.1 MATLAB Function for Processing SAR Data

```
function img = sar_lin(f,az_lin,iq_lin)


% INITIALIZATION

R=4*pi*f/3e8;% Transformation of Time Freqeuncy to Spatial Frequency
A=pi/180*az_lin;% Transformation of Angle in degree to radians
for j=1:147
A(j)=A(j)-2*pi;% Adjustment so that all angular values are between 0 and pi
end

% Initialization of Cartesian Grid
X=zeros(1,175);
Y=zeros(175,1);
for j=1:175
X(j)=208+(j-1);
Y(j)=208+(j-1);
end

val=zeros(175);% Initialize the matrix of values in the cartesian grid.



% INTERPOLATOR
```

[1] This content is available online at <http://cnx.org/content/m15665/1.1/>.

```
   for j=1:175

   j % Update on how far we are.

   for k=1:175

   r=sqrt(X(j)^2+Y(k)^2);
   a=atan(Y(k)/X(k));

   if (r>R(1) & r<R(512))

   % Data index of cartesian point
   J=ceil((r-R(1))*511/(R(512)-R(1)));
   K=ceil((a-A(1))*1540/(A(1541)-A(1)));

   % Linearly interpolate the cartesian point with its 4 nearest neighbor polar data
points.

   % Interpolate in R
   v0 = 1/(R(J+1)-R(J)) * ( iq_lin(J,K)*(R(J+1)-r) + iq_lin(J+1,K)*(r-R(J)) );
   v1 = 1/(R(J+1)-R(J)) * ( iq_lin(J,K+1)*(R(J+1)-r) + iq_lin(J+1,K+1)*(r-R(J)) );

   % Interpolate in THETA
   val(j,k) = 1/(A(K+1)-A(K)) * ( v0*(A(K+1)-a) + v1*(a-A(K)) );

   end

   end

   end


   % Plot the interpolated values
   figure(1)
   imagesc(abs(val));

   % Take the 2d inverse DFT to get the image
   img = ifft2(val);

   % Plot the image
   figure(2)
   imagesc(abs(img));
```

7.2 References

D. C. Munson Jr., J. D. O'Brien, W. K. Jenkins, "A Tomographic Formulation of Spotlight-Mode Synthetic Aperture Radar," Proc. IEEE, vol. 71, pp 917-925, August 1983.

D. C. Munson Jr., R. L. Visentin, "A Signal Processing View of Strip-Mapping Synthetic Aperture Radar," IEEE Transactions on Acoustics, Speech, and Signal Processing, vol. 37, no. 12, pp 2131-2147, December 1989.

G. D. Martin, A. W. Doerry, "SAR Polar Format Implementation with MATLAB," Sandia National Laboratories, SAND2005-7413, November 2005.

P. Buxa, L. Gorham, Lt. M. Lukacs, "Mapping of a 2D SAR Backprojection Algorithm to an SRC Reconfigurable Computing MAP Processor," Air Force Research Laboratory, Sensors Directorate.

Chapter 8

THE TEAM!![1]

Our Elec 301 group project team: THE LATE NIGHT ELECS
Aaron Hallquist: ahallquist@rice.edu
Tianlai Lu: tian@rice.edu
Max Magee: max.r.magee@rice.edu
Jason Ryan: jdr@rice.edu
Our pictures can be found on the right!

[1] This content is available online at <http://cnx.org/content/m15668/1.1/>.

Index of Keywords and Terms

Keywords are listed by the section with that keyword (page numbers are in parentheses). Keywords do not necessarily appear in the text of the page. They are merely associated with that section. *Ex.* apples, § 1.1 (1) **Terms** are referenced by the page they appear on. *Ex.* apples, 1

Attributions

Module: "Appendix and References"
By: Tianlai Lu
URL: http://cnx.org/content/m15665/1.1/
Pages: 23-25

Module: "THE TEAM!!"
By: Tianlai Lu
URL: http://cnx.org/content/m15668/1.1/
Page: 27

Tomographic Processing of Spotlight-Mode SAR
This collection explores spotlight-mode Synthetic Aperture Radar and analyzes raw SAR simulation data.

About Connexions
Since 1999, Connexions has been pioneering a global system where anyone can create course materials and make them fully accessible and easily reusable free of charge. We are a Web-based authoring, teaching and learning environment open to anyone interested in education, including students, teachers, professors and lifelong learners. We connect ideas and facilitate educational communities.

Connexions's modular, interactive courses are in use worldwide by universities, community colleges, K-12 schools, distance learners, and lifelong learners. Connexions materials are in many languages, including English, Spanish, Chinese, Japanese, Italian, Vietnamese, French, Portuguese, and Thai. Connexions is part of an exciting new information distribution system that allows for **Print on Demand Books**. Connexions has partnered with innovative on-demand publisher QOOP to accelerate the delivery of printed course materials and textbooks into classrooms worldwide at lower prices than traditional academic publishers.